The EMBO Journal (2010) 29, 559–573 | © 2010 European Molecular Biology Organization | All Rights Reserved 0261-4189/10
www.embojournal.org

THE EMBO JOURNAL

Molecular basis for antagonism between PDGF and the TGFβ family of signalling pathways by control of miR-24 expression

Mun Chun Chan[1], Aaron C Hilyard[1], Connie Wu[2], Brandi N Davis[2], Nicholas S Hill[3], Ashish Lal[4], Judy Lieberman[4], Giorgio Lagna[1] and Akiko Hata[1,2,*]

[1]Molecular Cardiology Research Institute, Tufts Medical Center, Boston, MA, USA, [2]Department of Biochemistry, Tufts University School of Medicine, Boston, MA, USA, [3]Pulmonary, Critical Care, and Sleep Division, Tufts Medical Center, Boston, MA, USA and [4]Immune Disease Institute and Program in Cellular and Molecular Medicine, Children's Hospital Boston, Harvard Medical School, Boston, MA, USA

Modulation of the vascular smooth-muscle-cell (vSMC) phenotype from a quiescent 'contractile' phenotype to a proliferative 'synthetic' phenotype has been implicated in vascular injury repair, as well as pathogenesis of vascular proliferative diseases. Both bone morphogenetic protein (BMP) and transforming growth factor-β (TGFβ)-signalling pathways promote a contractile phenotype, while the platelet-derived growth factor-BB (PDGF-BB)-signalling pathway promotes a switch to the synthetic phenotype. Here we show that PDGF-BB induces microRNA-24 (miR-24), which in turn leads to downregulation of Tribbles-like protein-3 (Trb3). Repression of Trb3 coincides with reduced expression of Smad proteins and decrease in BMP and TGFβ signalling, promoting a synthetic phenotype in vSMCs. Inhibition of miR-24 by antisense oligonuclotides abrogates the downregulation of Trb3 as well as pro-synthetic activity of the PDGF-signalling pathway. Thus, this study provides a molecular basis for the antagonism between the PDGF and TGFβ pathways, and its effect on the control of the vSMC phenotype.
The EMBO Journal (2010) **29,** 559–573. doi:10.1038/emboj.2009.370; Published online 17 December 2009
Subject Categories: signal transduction; differentiation & death
Keywords: BMP; microRNA; PDGF; TGFβ; vascular smooth-muscle cell

Introduction

During embryonic development, the transforming growth factor-β (TGFβ) and BMP pathways play multiple essential roles in the induction of ventral mesoderm (Davidson and Zon, 2000), cardiac myogenesis (Monzen *et al*, 2002; Schneider *et al*, 2003), vasculogenesis (Moser and Patterson, 2005), and angiogenesis. Targeted inactivation of BMP-signal transducers Smad1 and Smad5 produces a severe vascular phenotype (Moser and Patterson, 2005). TGFβ1- or TGFβ2-null mice die prematurely due to vascular defects. Proliferative and obliterative vascular diseases such as atherosclerosis, post-angioplasty restenosis, lymphangioleiomyomatosis (LAM), and pulmonary arterial hypertension (PAH) share common pathological characteristics, including abnormal proliferation and migration of vascular smooth-muscle-cells (vSMCs), and decrease in their ability to contract. In response to vascular injury, vSMCs undergo a unique process known as 'phenotype modulation': transition from a quiescent, 'contractile' phenotype to a proliferative, 'synthetic' state (Owens, 1995; Owens *et al*, 2004). Phenotypic plasticity is essential for vascular development and vascular remodelling after injury. However, an aberrant switch from a contractile to synthetic phenotype, characterized by proliferation and transformation into myofibroblasts, is a mechanism underlying the formation of plexiform lesions as well as various proliferative vascular disorders (Smith *et al*, 1990; Yi *et al*, 2000). It was shown that TGFβs and BMPs are able to inhibit vSMC proliferation and migration, and stimulate the expression of contractile vSMC markers, such as smooth-muscle α-actin (SMA), calponin-1 (CNN), and SM22α (SM22) (Misiakos *et al*, 2001; Guo *et al*, 2004; Lagna *et al*, 2007). Loss-of-function mutations of genes encoding receptors of TGFβs and BMPs have been linked to vascular disorders such as idiopathic PAH (IPAH) and hereditary hemorrhagic telangiectasia (ten Dijke and Arthur, 2007). Altogether, these results support the hypothesis that inhibition of TGFβ or BMP signalling plays an important role in the pathogenesis of proliferative and obliterative vascular diseases.

Unlike TGFβs and BMPs, platelet-derived growth factors (PDGFs) potently mediate a switch from a contractile to synthetic phenotype characterized by downregulation of vSMC marker gene expression as well as increased proliferation and migration (Owens *et al*, 2004; Lagna *et al*, 2007). Platelet-derived growth factor-BB (PDGF-BB) is able to counteract the contractile activity of TGFβ and BMP signalling, and inhibit contractile gene expression in vSMCs (Lagna *et al*, 2007). Elevated expression of proteins in the PDGF-signalling pathway is found in various cardiovascular disorders and vascular injuries, including atherosclerosis and restenosis (Andrae *et al*, 2008). PDGF released from platelets and endothelial cells at sites of vascular injury is thought to be a contributing factor to atherosclerosis (McNamara *et al*, 1996). Inhibition of PDGF signalling by the PDGF receptor (PDGFR) kinase inhibitor, imatinib mesylate (Gleevec) reduced atherosclerosis development, suggesting critical involvement of the PDGF pathway in vascular proliferative disorders (Andrae *et al*, 2008). However, the exact mechanism by which the PDGF pathway contributes to vascular disease remains unclear.

*Corresponding author. Molecular Cardiology Research Institute, Tufts Medical Center, 800 Washington Street, Box 8486, Boston, MA 02111, USA. Tel.: +1 617 636 0614; Fax: +1 617 636 5649;
E-mail: akiko.hata@tufts.edu

Received: 26 May 2009; accepted: 6 November 2009; published online: 17 December 2009

We recently reported that both TGFβ and BMP signals induce several small non-coding RNAs of the microRNA (miRNA) family, including miR-21, in vSMCs. miR-21 binds to the 3′-untranslated region (UTR) of programmed cell death-4 (PDCD4) mRNA, promoting degradation of PDCD4 mRNA and induction of vSMC contractile genes (Davis *et al*, 2008). The BMP pathway also activates the transcription of contractile genes by promoting nuclear translocation of two members of the myocardin (Myocd) family of transcription factors, MRTF-A and MRTF-B (Lagna *et al*, 2007), both potent transcription activators of vSMC-specific contractile genes containing CArG box (CC $(A/T)_6GG$) sequences in their promoter regions (Li *et al*, 2006; Kuwahara *et al*, 2007; Medjkane *et al*, 2009). In contrast, PDGF-BB suppresses the expression of Myocd or inhibits Myocd binding to the CArG box and abolishes vSMC gene transcription (Yoshida *et al*, 2007). Our study indicates that PDGF-BB also induces the expression of miR-221 (miR-221) in vSMCs (Davis *et al*, 2009). miR-221 targets the 3′-UTR of c-Kit and p27Kip1 mRNAs, and downregulates the expression of these proteins. Downregulation of c-Kit decreases Myocd protein and vSMC-specific genes, while downreguation of p27Kip1 promotes proliferation (Davis *et al*, 2009). Although TGFβ/BMP and the PDGF pathways have opposing effects on various aspects of vSMC phenotype modulation, direct crosstalk between these pathways has not been investigated. In this study, we demonstrate that PDGF-BB induces miR-24 (miR-24) in vSMCs. We show that miR-24 targets Tribbles-like protein-3 (Trb3) mRNA and downregulates its expression. Trb3 was previously identified as a protein that interacts with type-II BMP receptor (BMPRII) through a domain that is frequently mutated in familial IPAH patients (Chan *et al*, 2007). Trb3 promotes degradation of Smad ubiquitin-regulatory factor-1 (Smurf1), a negative regulator of BMP and TGFβ Smad-dependent signalling (Chan *et al*, 2007). In concurrence with our previous result, we find that PDGF-miR-24-mediated downregulation of Trb3 in vSMCs results in decreased Smad protein levels and vSMC contractile gene expression. Inhibition of miR-24 function in vSMCs prevents cells from switching to a synthetic phenotype upon PDGF-BB treatment. Thus, we propose that miR-24 is a key regulator of the crosstalk between the pro-contractile TGFβ/BMP signal and the pro-synthetic PDGF signal.

Results

PDGF-BB inhibits the BMP-mediated contractile phenotype

Human primary pulmonary smooth-muscle cells (PASMCs) were treated with BMP4 alone, PDGF-BB alone, or both BMP4 and PDGF-BB. The change in vSMC phenotype was evaluated by measuring the level of expression of vSMC-specific contractile gene markers, such as SMA, CNN and SM22; cell proliferation; and collagen lattice contraction.

As reported previously (Lagna *et al*, 2007), BMP4 induces SMA, CNN, and SM22, and PDGF-BB reduces their expression both at the mRNA (Figure 1A, top panel) and protein level (Figure 1A, bottom panel). When cells were treated with both BMP4 and PDGF-BB, no vSMC marker induction was observed, indicating an antagonism between BMP4 and PDGF-BB (Figure 1A, SMA, CNN, or SM22). Induction of a direct BMP target gene, *Id3*, whose expression was elevated ~4-fold after 6 h treatment with BMP4, was significantly reduced by co-stimulation with BMP4 and PDGF (Figure 1A, Id3).

The level of deformation (contraction) of collagen lattices can be affected by reorganization of actin or in response to contractile stimuli such as BMP4 in vSMCs (Neuman *et al*, 2009). To examine whether the change in vSMC markers shown in Figure 1A affects the contractility of the cells, PASMCs were treated with BMP4, PDGF-BB, or both for 24 h and the size of the collagen gel was measured 24 h after it was released from the culture plate wall. BMP4 treatment reduced the size of collagen lattice to 73%, indicating that BMP4 elevates collagen contraction, presumably through increased expression of contractile gene markers (Figure 1B). PDGF-BB treatment did not affect the gel size at a detectable level (Figure 1B). However, when PDGF-BB was added with BMP4, no significant contraction was observed (Figure 1B). Similarly, BMP4-induced cell growth inhibition (about 50%) was reversed by co-treatment with PDGF-BB (Figure 1C). Altogether, these results indicate that PDGF-BB exerts an antagonizing effect on the BMP pathway, potentially by affecting its basic signalling machinery.

Downregulation of Trb3 upon PDGF-BB stimulation

Trb3 can act as an important modulator of the BMP-signalling pathway by regulating the expression level of Smad signal-transducing proteins (Chan *et al*, 2007). Furthermore, changes in the level of Trb3 in vSMCs affects the vSMC phenotype (Chan *et al*, 2007). Therefore, we examined potential modulation of Trb3 upon PDGF-BB stimulation. In a time-course experiment, we monitored the change in Trb3 mRNA by semi-quantitative RT–PCR (qRT–PCR) upon PDGF-BB or BMP4 treatment in PASMCs (Figure 2A). Trb3 mRNA decreased after 8 h and stayed low up to 72 h after PDGF-BB treatment (Figure 2A, and data not shown). BMP4 treatment alone had no effect on Trb3 mRNA expression (Figure 2A). In agreement with the mRNA level, Trb3 protein was reduced by PDGF-BB treatment after 4 h and further reduced after 24 h in PASMCs (Figure 2B). Immunofluorescence staining of PASMCs indicated that PDGF-BB reduces the expression of Trb3 and of the contractile marker SMA (Figure 2C). Downregulation of Trb3 protein and mRNA by PDGF was also confirmed in the rat PASMC line PAC1 (Supplementary Figure S1). We previously reported that downregulation of Trb3 results in reduction of Smad signal transducers for both the BMP- and TGFβ-signalling pathway (Chan *et al*, 2007). We examined whether PDGF-BB treatment reduces BMP-specific Smad1 (Figure 2D, left panel) or TGFβ-specific Smad2 and Smad3 (Figure 2D, right panel) by immunoblot analysis. BMP4 or TGFβ treatment did not significantly affect Trb3 or Smad levels (Figure 2D). PDGF-BB stimulation, however, dramatically reduced both Trb3 and Smad protein (Figure 2D). Anti-phospho-Smad1/5 or anti-phospho-Smad2 antibody immunoblots indicate robust induction of phosphorylation of Smads upon BMP4 or TGFβ treatment (Figure 2D). Co-treatment with PDGF-BB and BMP4 or TGFβ resulted in significant reduction in phospho-Smad levels, due to decreased total Smad protein (Figure 2D). These results suggest that PDGF-BB may in part antagonize the BMP or TGFβ pathways by decreasing Trb3 expression, which leads to downregulation of Smad signal transducers.

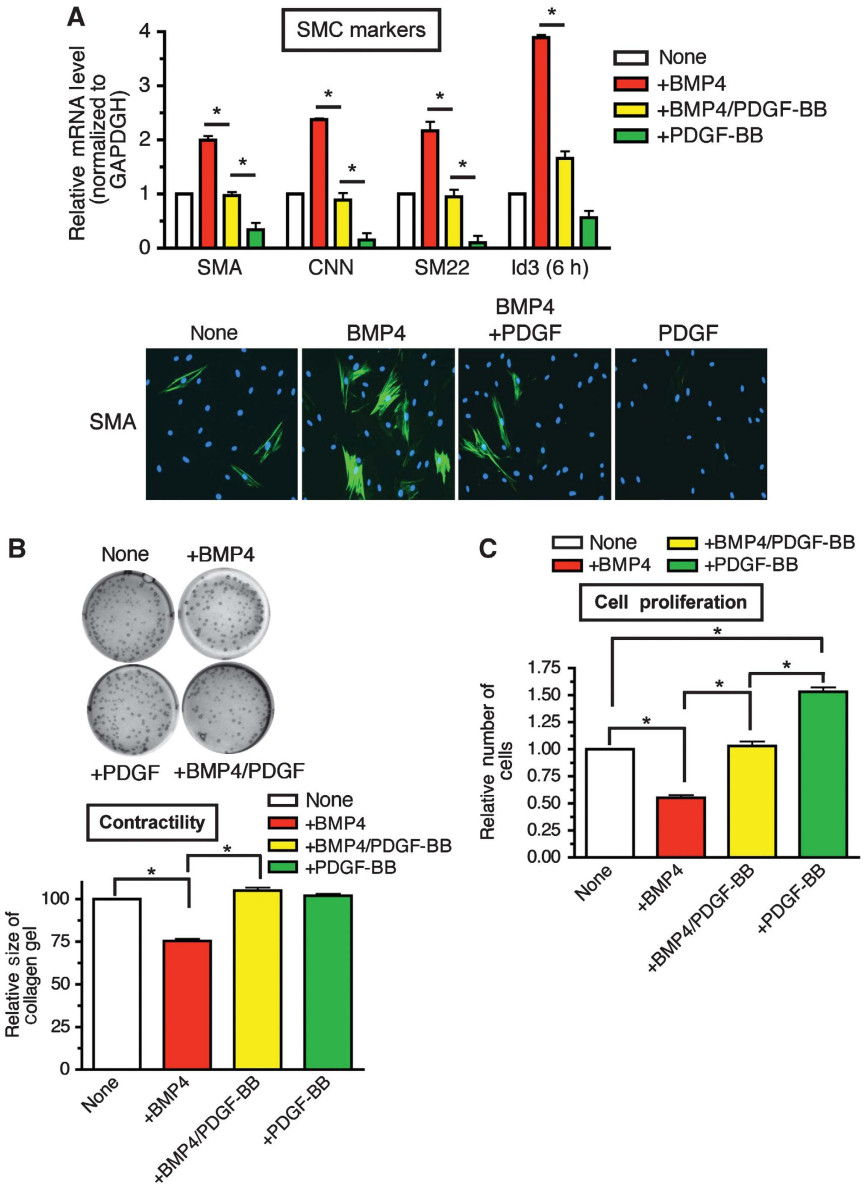

Figure 1 PDGF-BB inhibits BMP-mediated contractile phenotype in PASMCs. (**A**) Human PASMCs were treated with 3 nM BMP-4 alone (+BMP4), both 3 nM BMP4 and 20 ng/ml PDGF-BB (+BMP4/PDGF-BB), or 20 ng/ml PDGF-BB alone (+PDGF-BB) for 24 h (for vSMC markers) or 6 h (for Id3), followed by qRT–PCR (top panel) and immunofluorescence staining (bottom panel). The relative mRNA levels of vSMC markers SMA, CNN, or SM22, as well as the BMP-target gene Id3, were examined by qRT–PCR. Results were normalized to GAPDH expression, and the relative mRNA levels are presented as means ± s.e.m., with each experiment conducted in triplicate ($n=3$) (top panel). The difference between two results indicated by asterisks is statistically significant; $^*P<0.001$. Immunofluorescence staining was performed with FITC-conjugated anti-SMA antibody (green) and by DAPI staining (blue) (bottom panel). (**B**) PASMCs were treated with 3 nM BMP4, 20 ng/ml PDGF-BB, or both for 24 h prior to being embedded to collagen gel lattices. Twenty-four hours after the collagen lattices were dissociated from the dish, gel contraction was photographed by using a digital camera (top panel). The area of the gel lattices was determined with the ImageJ software, and the relative lattice area was obtained by dividing the area at each time point by the initial area of the well (bottom panel). Experiments were performed three times. Data represent the means ± s.e.m.; $^*P<0.01$. (**C**) PASMCs were starved for 24 h, followed by treatment with BMP4, PDGF-BB, or both for 48 h. Cells were tryspinized and counted using a haemocytometer. The relative number of cells compared with untreated cells was plotted as means ± s.e.m. ($n=3$); $^*P<0.01$.

Trb3 is a novel target of miR-24

Next we investigated the mechanism by which PDGF-BB downregulates Trb3. The activity of a *Trb3* promoter–luciferase-reporter construct, which contains a ~1.9-kb region of the human Trb3 gene promoter (Ohoka *et al*, 2005), was not affected by PDGF-BB treatment (Supplementary Figure S2A). Furthermore, the transcription rate of Trb3 gene was not altered by PDGF treatment (Supplementary Figure S2B). It is likely that PDGF-BB controls Trb3 mRNA level through a mechanism other than transcriptional regulation. As an alternative mechanism, we examined miRNA-mediated downregulation of *Trb3*. Computational analysis by TargetScan5.1 predicted that the 3′-UTR of the *Trb3* transcript contains an 8-mer miR-24 seed sequence at a position 78–84 nucleotides after the stop codon, which is phylogenetically conserved among mammals (Figure 3A, upper panel). To examine whether miR-24 can downregulate Trb3 mRNA expression in vSMCs, three different doses of chemically

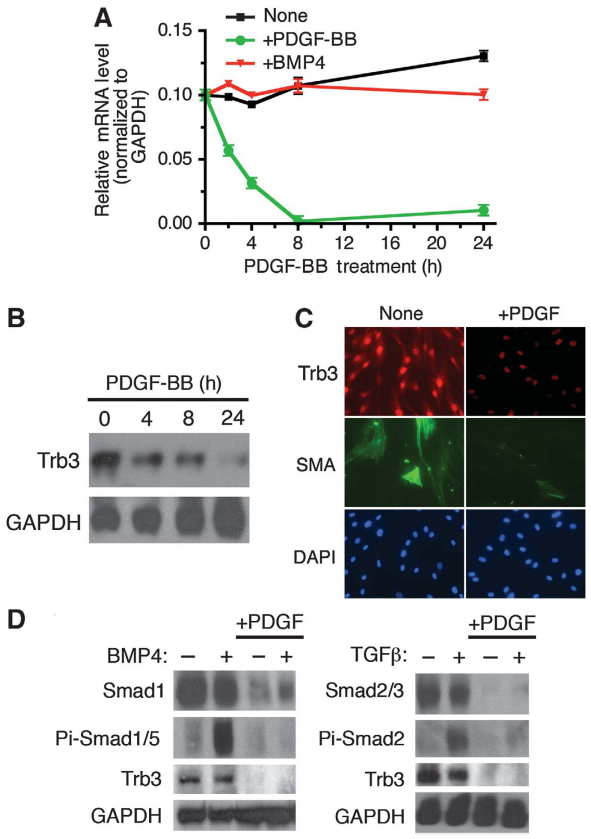

Figure 2 PDGF-BB stimulation decreases Trb3 expression. (**A**) PASMCs were stimulated with 3 nM BMP-4 or 20 ng/ml PDGF-BB for 2, 4, 8, or 24 h and subjected to qRT–PCR analysis. Relative expression of Trb3 mRNA normalized to GAPDH is plotted. (**B**) PASMCs were treated with 20 ng/ml PDGF-BB for 4, 8, or 24 h. Cells were harvested and subjected to immunoblot analysis using anti-human Trb3 antibody and anti-GAPDH antibody used as loading control. The results are representative of three independent experiments. (**C**) PASMCs were treated with 20 ng/ml PDGF-BB for 24 h and then subjected to immunofluorescence staining using anti-hTrb3 antibody conjugated to Cy3 (red), anti-SMA antibody conjugated to FITC (green), and by DAPI staining (blue). (**D**) Whole-cell lysates from PASMCs treated with 3 nM BMP4 or 100 pM TGFβ1 for 0.5 h, 20 ng/ml PDGF-BB for 4 h, or stimulated with PDGF-BB for 4 h followed by BMP4 or TGFβ1 for 0.5 h were subjected to immunoblot analysis using anti-Smad1, anti-Smad2/3, anti-phospho-Smad-1/5 (Pi-Smad1/5), or anti-phospho-Smad2 (Pi-Smad2) antibody; anti-hTrb3 antibody; or anti-GAPDH antibody (loading control). The experiment was repeated twice, with similar results.

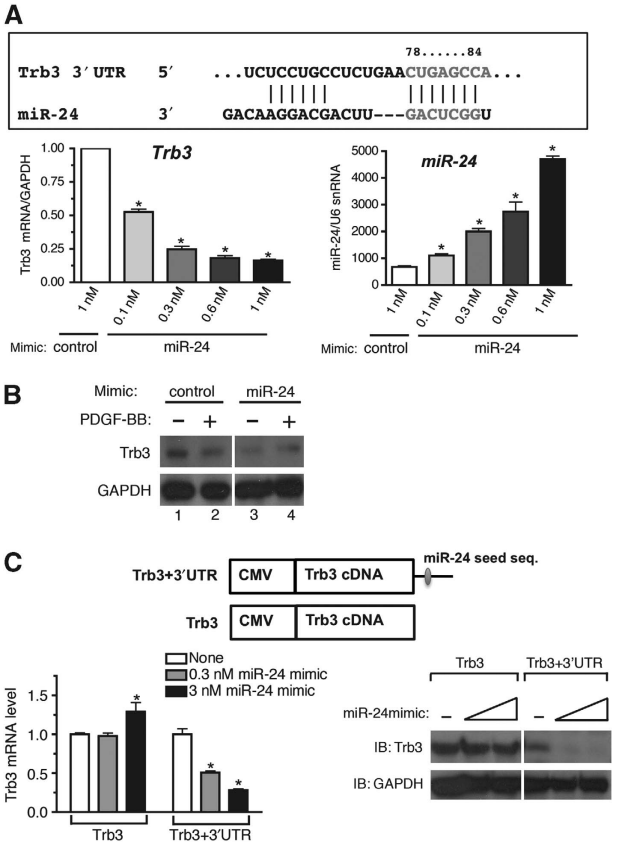

Figure 3 miR-24 leads to downregulation of Trb3. (**A**) A schematic representation of the miR-24-targeting site in the 3′-UTR Trb3 transcripts (top panel). The conserved 8-mer seed sequence is shown in grey. PASMCs were transfected with 1 nM non-specific (GFP) mimic (control) or increasing amounts (0.1, 0.3, 0.6, or 1 nM) of chemically modified, synthetic miR-24 oligonucleotides (miR-24 mimic). Twenty-four hours after transfection of mimic, cells were harvested and subjected to qRT–PCR analysis. Relative Trb3 mRNA level normalized to GAPDH (bottom left), as well as levels of mature miR-24 normalized to U6 snRNA (bottom right), is plotted as means ± s.e.m. ($n=3$); $^*P<0.001$ (versus the expression levels of control-transfected PASMCs). (**B**) PASMCs were transfected with 0.3 nM control mimic or 0.3 nM miR-24 mimic. Twenty-four hours after transfection of mimic, cells were stimulated with 20 ng/ml PDGF-BB for 6 h and subjected to immunoblot analysis with anti-hTrb3 antibody or anti-GAPDH antibody (loading control). The experiment was repeated three times, with similar results. (**C**) Cos7 cells were transfected with a construct carrying the human Trb3 cDNA construct with the 3′-UTR, which includes the miR-24 seed sequence (Trb3 + 3′-UTR) or deleted in the 3′-UTR (Trb3), with increasing amounts of miR-24 mimic (0.3 or 3 nM). Cells were harvested and subjected to qRT–PCR analysis (left panel) and immunoblot analysis (right panel). Relative Trb3 mRNA expression normalized to GAPDH is plotted ($n=3$); $^*P<0.001$ (compared with no miR-24 mimic transfection (white bar) of each set). Immunoblot analysis was performed using anti-hTrb3 antibody and anti-GAPDH antibody used as loading control. The immunoblot presented is representative of three independent experiments. A full-colour version of this figure is available at *The EMBO Journal* Online.

modified, synthetic miR-24 oligonucleotides (miR-24 mimic) were transfected into PASMCs, followed by qRT–PCR analysis of Trb3 mRNA. Increasing amounts of miR-24 mimic (about 1.6, 3.0, 4.0, and 7.0 times the endogenous miR-24 level) were expressed in PASMCs (Figure 3A, right panel). Under these conditions, Trb3 mRNA level was reduced to an average of 52, 24, 18, and 16% of the basal level, respectively (Figure 3A, left panel), suggesting that miR-24 targets Trb3 mRNA and leads to its degradation. Next, miR-24 mimic or control mimic were transfected into PASMCs, followed by 24-h PDGF-BB treatment and Trb3 protein immunoblot analysis. The miR-24 mimic alone significantly reduced Trb3 protein to a level lower than that in PDGF-BB-treated cells with the control mimic (Figure 3B, lanes 2 and 3). In the presence of miR-24 mimic, PDGF-BB did not further reduce Trb3 (Figure 3B, lanes 3 and 4). To examine whether miR-24 targets the predicted miR-24 seed sequence in the 3′-UTR of Trb mRNA, a Trb3 cDNA expression construct with or without the 3′-UTR sequence was generated (Figure 3C, top panel) and transfected into Cos7 cells. The effect of miR-24 mimic on the expression of the two different constructs was examined by qRT–PCR and immunoblot analyses. As shown in Figure 3C, miR-24 mimic dose dependently suppressed both mRNA (Figure 3C, left panel) and protein (Figure 3C, right

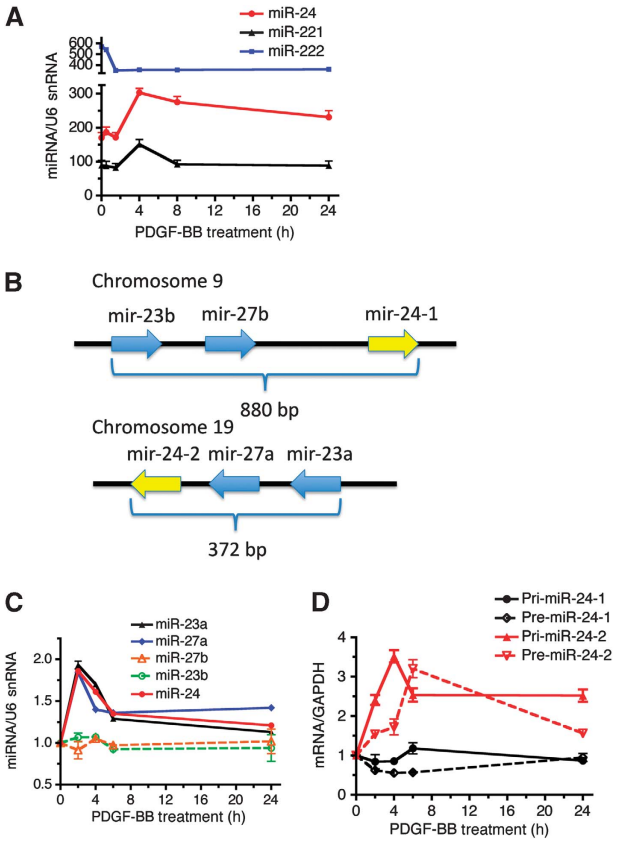

Figure 4 PDGF-BB induces miR-24 expression. (**A**) PASMCs were stimulated with 20 ng/ml of PDGF-BB for 1, 2, 4, 8, or 24 h, followed by qRT–PCR to determine the expression of miR-24, miR-221, and miR-222. The expression of individual miRNA normalized to U6 snRNA is plotted (means ± s.e.m., $n = 3$). (**B**) A schematic representation of the miR-24-1 gene cluster on human chromosome-9, which includes miR-23b and miR-27b, and the miR-24-2 gene cluster on human chromosome-19, which includes miR-27a and miR-23a. (**C**) PASMCs were treated with PDGF-BB for 2, 4, 6, or 24 h, followed by qRT–PCR analysis using primers for miR-23a, miR-27a, miR-27b, miR-23b, or miR-24. The time-course change in the expression of miRNA normalized to U6 snRNA after PDGF-BB stimulation is plotted (means ± s.e.m., $n = 3$). (**D**) PASMCs were treated with PDGF-BB for 2, 4, 6, or 24 h, followed by qRT–PCR analysis of primary transcripts of miR-24-1 (Pri-miR-24-1), primary transcripts of miR-24-2 (Pri-miR-24-2), intermediate products of miR-24-1 (Pre-miR 24-1), and intermediate products of miR-24-2 (Pre-miR-24-2). The time-course change in the expression of RNAs was normalized to GAPDH and plotted (means ± s.e.m., $n = 3$).

panel) expression from the construct containing the 3′-UTR (Figure 3C, Trb3 + 3′-UTR). No change in Trb3 mRNA or protein was observed when the 3′-UTR was missing (Figure 3C, Trb3), indicating that the 3′-UTR, and presumably the miR-24 seed sequence contained in it, is essential for downregulation of Trb3 by miR-24.

PDGF-BB induces miR-24-2 transcription

We speculated that PDGF-BB might downregulate Trb3 by inducing the expression of miR-24 in PASMCs. We recorded a time-course profile of the expression of miR-24 as well as miR-221, which was previously found to be induced by PDGF-BB (Davis *et al*, 2009), in PASMCs after PDGF-BB treatment (Figure 4A, black line). miR-222 serves as a negative control as its expression is not regulated by PDGF-BB (Davis *et al*, 2009) (Figure 4A, blue line). miR-24 was induced about 1.5-fold 4 h after PDGF-BB treatment and remained above the basal level up to 24 h, similar to miR-221 (Figure 4A, red line). This is consistent with the result that Trb3 mRNA level decreases to approximately 25% of the basal level within 4 h after PDGF-BB treatment (Figure 2A). The miR-24 gene is encoded in a gene cluster comprising miR-27 and miR-23 within a genomic region of less than 900 bp. There are two copies of the miR-24 gene cluster; one located on chromosome-9 (miR-24-1 gene cluster, encoding miR-24-1, miR-23b, and miR-27b) and the other on chromosome-19 (miR-24-2 gene cluster, coding for miR-24-2, miR-23a, and miR-27a) (Figure 4B). The sequences of miR-24-1 and miR-24-2 are identical and indistinguishable by qRT–PCR analysis, while sequences of miR-23a and miR-23b, or miR-27a and miR-27b are different. To determine whether both miR-24-1 and miR-24-2 are similarly regulated by PDGF-BB, the levels of the two variants of miR-23 and miR-27 were examined individually by qRT–PCR (Figure 4C). The miRNAs in the miR-24-2 gene cluster (miR-23a and miR-27a) were induced ~2-fold by PDGF-BB, similar to miR-24 (Figure 4C). By contrast, miR-23b (Figure 4C, green dotted line) and miR-27b (Figure 4C, orange dotted line) were not altered by PDGF-BB treatment. These results indicate that the miR-24-2 cluster, but not miR-24-1 cluster, is regulated by PDGF-BB. To examine which step of miR-24-2 biogenesis is regulated by PDGF-BB, we examined the level of miR-24 primary transcripts (Pri-miR-24-2) and the first processing product (Pre-miR-24-2) after PDGF-BB treatment. These precursor RNAs are sufficiently distinct for miR-24-1 and miR-24-2 to be distinguishable by RT–PCR. Induction of both Pri-miR-24-2 (~3.5 fold) and Pre-miR-24-2 (~3.2-fold) was observed within 2–4 h after PDGF treatment, suggesting that the miR-24-2 gene cluster is regulated by the PDGF pathway at the transcriptional level (Figure 4D, red solid and dotted lines). The expression of neither Pri-miR-24-1 nor Pre-miR-24-1 was altered by PDGF-BB treatment (Figure 4D, black solid and dotted lines), confirming that PDGF-BB does not modulate the expression of the miR-24-1 gene cluster.

miR-24 is a critical mediator of the pro-synthetic activity of PDGF-BB

To investigate the potential role of miR-24 in the PDGF-mediated downregulation of Trb3, 2′-*O*-methyl-modified RNA oligonucleotides complementary to the miR-24 sequence (anti-miR-24) were transfected into PASMCs to inhibit endogenous miR-24, and the levels of Trb3 and the vSMC marker SMA were examined. Transfection of 50 nM anti-miR-24 decreased endogenous miR-24 level by approximately 60% (Figure 5A, right panel). Induction of miR-24 by PDGF-BB was significantly reduced by anti-miR-24 transfection in comparison with cells transfected with control oligonucleotides (anti-GFP) (Figure 5A, right panel). In control cells, PDGF-BB treatment decreased Trb3 mRNA expression by approximately 50% (Figure 5A, left panel). In anti-miR-24-transfected cells, however, the level of Trb3 was slightly increased (~10%) as compared with the basal level and not significantly decreased by PDGF-BB, suggesting that PDGF-BB is unable to downregulate Trb3 when expression of endogenous miR-24 is impaired (Figure 5A, left panel). Similarly, the ability of PDGF-BB to reduce SMA expression was decreased in the presence of anti-miR-24 (Figure 5A, left panel). These results indicate that miR-24 plays a critical

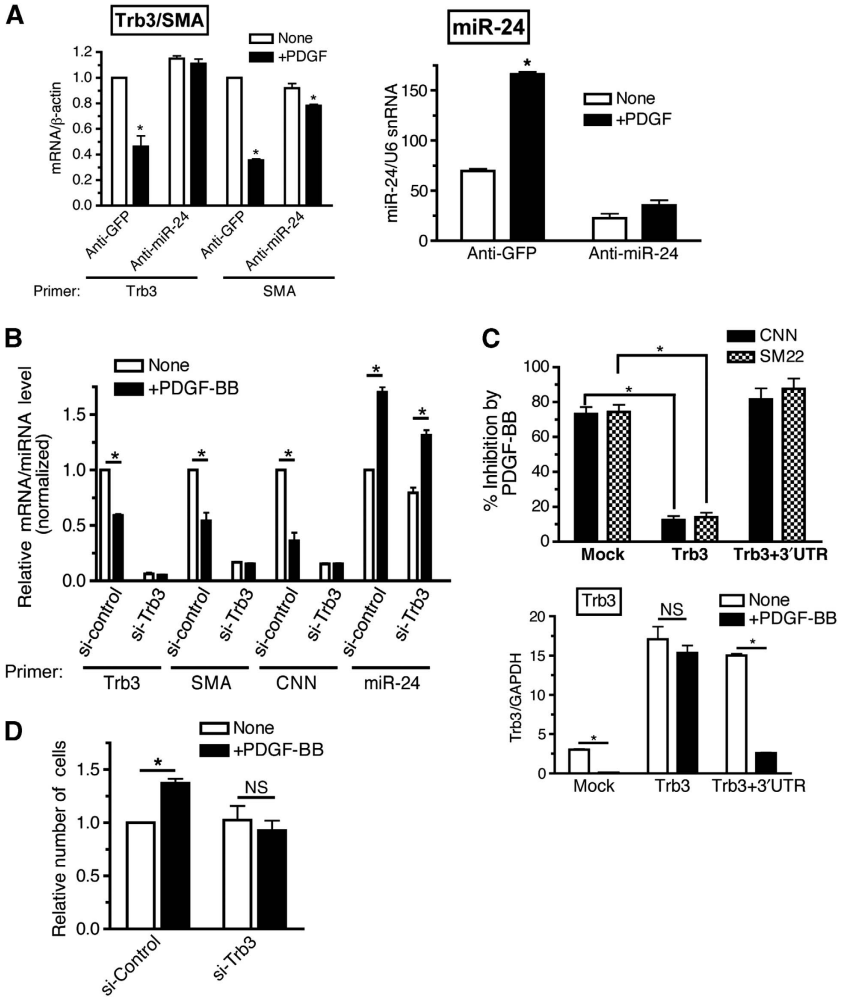

Figure 5 miR-24 expression is crucial for PDGF-BB downregulation of Trb3. (**A**) PASMCs were transfected with 50 nM control antisense (anti-GFP) or anti-miR-24 (anti-miR-24), followed by stimulation with or without 20 ng/ml of PDGF-BB (+PDGF) for 24 h. qRT–PCR analysis was performed and relative expression of Trb3 or SMA mRNA normalized to β-actin (left panel) and miR-24 expression normalized to U6 snRNA expression (right panel) was also examined and plotted as means ± s.e.m. ($n=3$); $^*P<0.001$ (compared with unstimulated sample transfected with the same anti-miR). (**B**) PASMCs were transfected with 50 nM non-targeting control siRNA (si-Control) or siRNA against human Trb3 (si-Trb3) for 24 h, followed by stimulation with 20 ng/ml PDGF-BB (+PDGF-BB) for 24 h. Relative expression of Trb3, SMA, or CNN normalized to GAPDH and miR-24 expression normalized to U6 snRNA is plotted (means ± s.e.m., $n=3$; $^*P<0.001$). (**C**) Rat PAC1 cells were transfected with a construct carrying the human Trb3 cDNA construct with the 3′-UTR (Trb3 + 3′-UTR) or deleted in 3′UTR (Trb3), followed by stimulation with 20 ng/ml PDGF-BB (+PDGF-BB) for 24 h. Percent inhibition of CNN or SM22 mRNA level upon PDGF treatment is plotted (top panel). Relative expression of both endogenous rat Trb3 and exogenous human Trb3 mRNA normalized to GAPDH is plotted (bottom panel) as means ± s.e.m. ($n=3$); $^*P<0.001$. (**D**) PASMCs were transfected with 50 nM si-Control or si-Trb3 for 24 h, followed by treatment with PDGF-BB for 48 h. Cells were tryspinized and counted using a haemocytometer. The relative number of cells compared with untreated cells is plotted as means ± s.e.m. ($n=3$); $^*P<0.01$.

role in the regulation of Trb3 and vSMC genes by PDGF-BB. To investigate whether other targets of miR-24, besides Trb3, are involved in PDGF-BB-mediated downregulation of vSMC genes, Trb3 was silenced by small interfering RNA (siRNA) (si-Trb3) in PASMCs (Figure 5B). Transfection of si-Trb3 reduced endogenous Trb3 mRNA expression to 5% of that of the control (Figure 5B). miR-24 was induced similarly by PDGF-BB treatment both in si-Trb3 cells and si-Control cells (Figure 5B). PDGF-BB-mediated downregulation of SMA and CNN was observed in si-Control cells but not in si-Trb3 cells (Figure 5B, left panel), suggesting that Trb3 is required for the PDGF-BB-mediated decrease in contractile gene expression. To further confirm a critical role of the PDGF–miR-24–Trb3 axis, Trb3 expression constructs with or without the 3′-UTR (see Figure 3C, top panel) were transfected prior to PDGF treatment and the effect of PDGF on contractile markers *CNN* and *SM22* was examined in PAC1 cells (Figure 5C). If PDGF suppresses *SM22* through miR-24-mediated downregulation of Trb3, it is expected that only the Trb3 construct missing the 3′-UTR (Trb3), which is resistant to miR-24, is able to rescue *SM22* and *CNN* expression. Similar levels of expression of Trb3 from the construct with or without 3′-UTR (~5-fold over the endogenous level) were observed at the basal state (Figure 5C, bottom panel). Both Trb3 constructs elevated the basal expression of both *CNN* and *SM22* about two- three-fold (Supplementary Figure S5). Unlike the Trb3 construct with the 3′-UTR (Trb3 + 3′-UTR), the Trb3 construct deleted in 3′-UTR (Trb3) was able to reduce the level of inhibition of *CNN* and *SM22* by PDGF (Figure 5C, top panel), confirming that the PDGF-mediated miR-24–Trb3-regulatory pathway plays a critical role in the pro-synthetic effect of PDGF-BB. Next a potential role of miR-24-mediated downregulation of

Trb3 in PDGF-mediated cell growth regulation was examined. In control cells (si-Control), PDGF-BB treatment promoted proliferation of PASMCs (Figure 5D). When endogenous Trb3 level was downregulated by si-Trb3, the proliferative effect of PDGF-BB treatment was attenuated, suggesting that Trb3 is required not only for PDGF-mediated contractile gene regulation, but also for its cell-proliferative effect (Figure 5D). Altogether, these results support that the miR-24¡Trb3 axis is essential for the pro-synthetic activity of PDGF-BB.

miR-24 antagonizes BMP4 signals

We previously proposed that Trb3 stabilizes Smad1/5 proteins by promoting proteasome-dependent degradation of Smurf1, which is an E3 ubiquitin ligase for Smads (Chan *et al*, 2007). Therefore, we hypothesized that miR-24 inhibits the BMP–Smad pathway through downregulation of Trb3 and Smads. Overexpression of miR-24 in PASMCs decreased both Trb3 and Smad1 protein levels and abolished BMP4-mediated phosphorylation of Smad1/5 proteins (Figure 6A), similar to the effect of PDGF-BB treatment (see Figure 2D), suggesting that miR-24 is able to inhibit the BMP–Smad pathway in PASMCs. Next the inhibitory effect of miR-24 on the BMP–Smad pathway was further demonstrated by examining the expression of various transcriptional and post-transcriptional targets of BMP–Smads after transfection of miR-24 mimic or control (GFP) mimic. Transfection of 0.3 nM miR-24 mimic into PASMCs elevated the miR-24 level ~2-fold over the endogenous level (Figure 6B, miR-24) and reduced Trb3 mRNA to 30% of the endogenous level (Figure 6B, Trb3). In the presence of miR-24 mimic, induction of both vSMC-specific BMP targets SMA and CNN, and the non-vSMC-specific BMP target Id3 was significantly reduced as compared with that in control mimic-transfected cells, although not completely abolished (Figure 6B). To confirm that the miR-24-mediated inhibition of BMP activity on SMA and Id3 is due to downregulation of Trb3 and its function, PASMCs transfected with miR-24 mimic were infected with adenovirus carrying either wild-type Trb3 (Trb3 (WT)) cDNA or a Trb3 mutant cDNA deleted in amino acids 239–266 (Trb3 (ΔK)), which is unable to promote degradation of Smurf1, and therefore unable to positively modulate BMP signalling (Chan *et al*, 2007). Both Trb3 constructs are deleted in the 3′-UTR and therefore resistant to the miR-24 mimic (Figure 6C, bottom left panel). Both Trb3 (WT) and Trb3 (ΔK) were expressed at similar levels (Figure 6C, bottom left panel), and expression of Trb3 had no effect on miR-24 mimic expression (Figure 6C, bottom right panel). Similar to the result in Figure 6B, transfection of miR-24 mimic inhibited the induction of SMA and Id3 by BMP4 (Figure 6C, top panel). Exogenous Trb3 (WT) abolished the inhibitory effect of miR-24 mimic and rescued the BMP4-mediated induction of SMA and Id3, confirming the essential role of the miR-24–Trb3 axis in the regulation of the BMP pathway (Figure 6C, top panel). In contrast Trb3 (ΔK) was not able to inhibit the effect of miR-24 mimic (Figure 6C, top panel). Thus, these results support our hypothesis that miR-24 inhibits the BMP–Smad-signalling pathway through downregulation of Trb3.

Our previous study demonstrated that Smad proteins control miR-21 biosynthesis at the first processing step by Drosha microprocessor complex, which results in miR-21 (Davis *et al*, 2008) induction of about two-fold by BMP4 or TGFβ. Therefore, we speculated that miR-24-mediated downregulation of Trb3 and Smad may affect the regulation of miR-21 synthesis by BMP4. Overexpression of miR-24 abolished the BMP4-mediated induction of miR-21 (Figure 6D). Downregulation of Trb3 by siRNA (si-Trb3) phenocopied the effect of miR-24 mimic and abolished miR-21 induction by BMP4 (Figure 6E). These results indicate that miR-24 negatively regulates both transcriptional and non-transcriptional functions of BMP–Smads through a mechanism involving predominantly downregulation of Trb3. In agreement with these results, we observed that PDGF-BB treatment reduces miR-21 expression, presumably as a result of induction of miR-24 (Supplementary Figure S3). We next examined whether miR-24 expression affects other BMP4 responses in vSMCs, such as cell growth suppression (Lagna *et al*, 2007) and induction of actin remodelling (Neuman *et al*, 2009). miR-24 mimic expression abolished the BMP4-mediated cell growth inhibition in PASMCs (Figure 6F). Similarly, contraction of PASMCs in a collagen lattice in response to BMP4-induced actin remodelling was inhibited by miR-24 mimic (Figure 6G). Altogether, these results suggest that miR-24 can interfere with different pro-contractile activities of the BMP4 pathway in vSMCs.

To examine whether inhibition of the BMP–Smad pathway by miR-24 is cell-type-specific, a clone of the mouse embryonal carcinoma P19 cell line stably transformed with the BMP target gene promoter–luciferase reporter (BRE-Luc) (Ku *et al*, 2005) was transfected with miR-24 mimic, control (GFP) mimic, or si-Trb3, and stimulated with BMP4 (Figure 6H). In comparison with control cells, increasing amounts of miR-24 mimic decreased the response of BRE-Luc to BMP4 (Figure 6H). At the highest dose of miR-24 mimic, the response of BRE-Luc was similar to that elicited in si-Trb3-transfected cells (Figure 6H). Finally, we measured the effect of miR-24 on BMP4/Smad-mediated osteoblastic differentiation of mouse myoblast C2C12 cells, which is characterized by induction of the osteoblast marker alkaline phosphatase (ALP). When miR-24 was overexpressed in C2C12 cells, BMP4-mediated ALP induction was reduced by half, suggesting that miR-24 antagonizes the ability of BMP4 to promote osteoblast differentiation (Figure 6I). Trb3 level was decreased to 35% and induction of the BMP target gene Id3 was decreased to half in miR-24 mimic-expressing cells, suggesting that the miR-24–Trb3–Smad axis blocks osteoblast differentiation. Thus, we conclude that miR-24 antagonizes the BMP–Smad-signalling pathway both in vSMCs and non-vSMCs.

Next, we addressed whether miR-24 plays an essential role in inhibition of pro-contractile BMP activity by PDGF-BB. PASMCs were transfected with anti-miR-24 or anti-GFP (control), followed by treatment with BMP4 alone or BMP4 and PDGF-BB. In control cells, PDGF-BB blocked the induction of vSMC markers by BMP4 (Figure 7A, anti-GFP). When miR-24 activity was inhibited by anti-miR-24, however, PDGF-BB was unable to inhibit the BMP4-mediated induction of contractile genes (Figure 7A, anti-miR-24). Similar results were obtained by examining the effect of PDGF-BB on other pro-contractile signals by BMP4, such as cell growth inhibition (Figure 7B) and induction of cell contraction (Figure 7C). Altogether, these results demonstrate that miR-24 induction is essential for the ability of PDGF-BB to antagonize the pro-contractile BMP4 signals.

Hypoxia induces miR-24 and downregulation of Trb3 and BMP signal

It has been shown that the Trb3 level is altered by various pathological or physiological conditions (Bowers *et al*, 2003; Qi *et al*, 2006). Therefore, we examined a possible change in Trb3 protein and miR-24 expression in lung and pulmonary artery (PA) samples using a rat hypoxia-induced PAH model. qRT–PCR analysis demonstrated that the levels of Trb3 and vSMC markers in hypoxia-treated lung samples were reduced to about 40–50% of that in normoxia-treated control lung samples (Figure 8A, top panel). Conversely, miR-24 level was elevated about two-fold in hypoxia-treated samples in

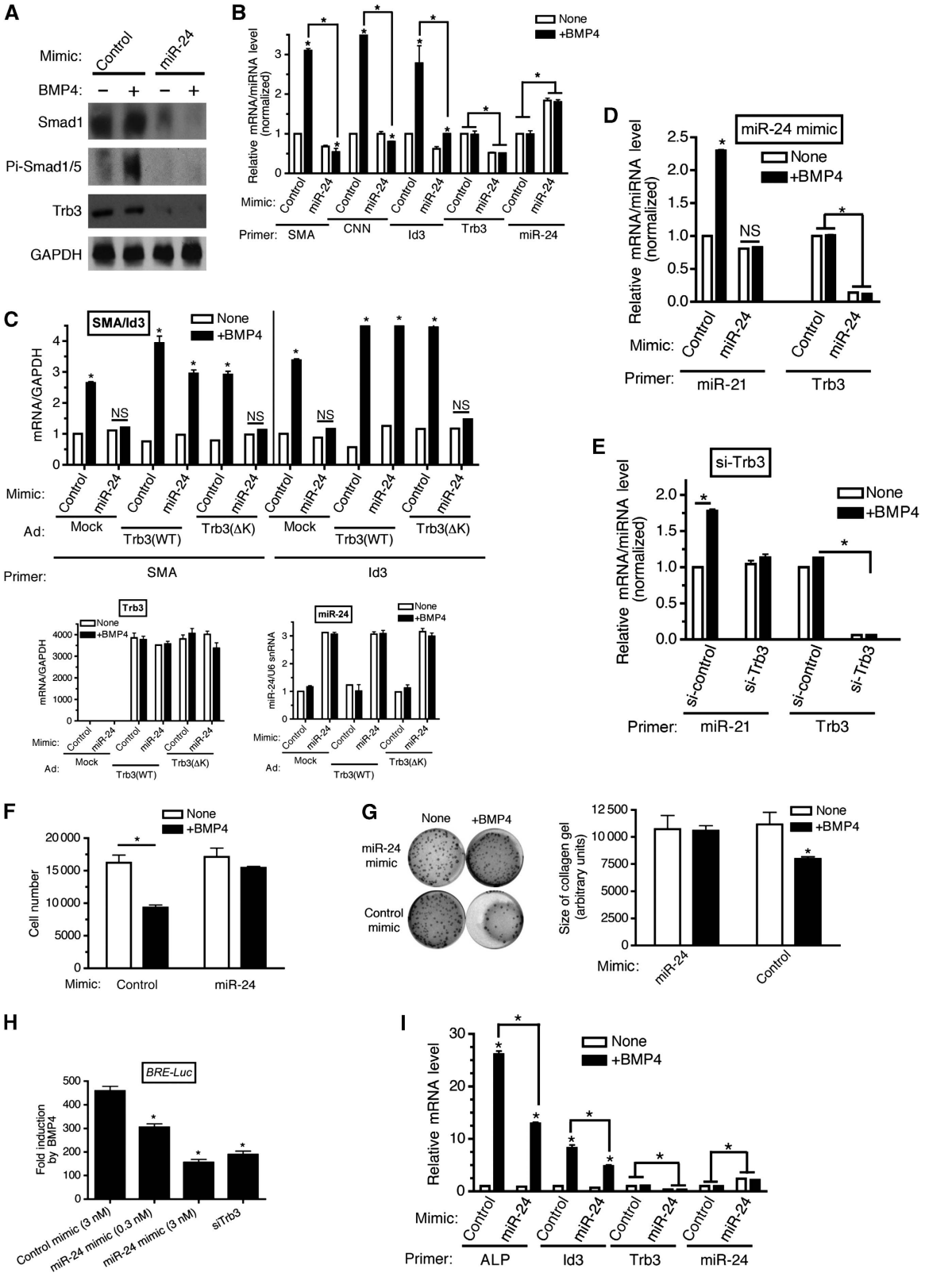

comparison with that in control samples (Figure 8A, bottom panel). miR-221, which was previously shown to be induced by the PDGF-signalling pathway, similar to miR-24 (Davis *et al*, 2009), was also increased about 1.5-fold after hypoxia treatment, while the level of an unrelated miRNA, miR-100, was unchanged (Figure 8A, bottom panel). Immunohistochemical analysis of SMA demonstrated that the medial layer of hypoxic rat PAs is thicker than that of a control (normoxic) rat due to overproliferation of vSMCs, which is characteristic of PAs of patients with PAH (Figure 8B). Phospho-Smad1/5/8 staining was detected in the medial layer of normoxic PAs (Figure 8B). At higher magnification, much of phospho-Smad1/5/8 staining had nuclear localization, suggesting that the BMP signal is active in those cells (Figure 8B). Consistent with a previous report (Yang *et al*, 2005), dramatically reduced staining of total Smad1 and phospho-Smad1/5/8 was observed in hypoxic rat PAs, suggesting a decrease in BMP signalling in these cells (Figure 8B). Reduced expression of Trb3 was also observed in the media layer of the PAs from rats subjected to hypoxia (Figure 8B). To examine whether the decrease in Trb3 protein level in hypoxic PAs is due to a change in miR-24 expression, the same samples were probed for miR-24 expression by a fluorescence *in situ* hybridization (FISH) using fluorescein isothiocyanate (FITC)-conjugated anti-miR-24 probes (Figure 8C, top two panels, green). Quantitative analysis of miR-24 staining indicates that the media of the hypoxia-treated sample expresses a twofold higher level of miR-24 as compared with the normoxic media, after normalization for the different medial areas in the two samples (Figure 8C, top two panels), indicating that miR-24 expression is modulated by vascular injury in the vSMC layer *in vivo*. The complementary patterns of expression of Trb3 and miR-24 in the media of PAs, as well as in lung samples from normoxia or hypoxia-treated rat, strongly support the hypothesis that elevated expression of miR-24 leads to downregulation of Trb3 *in vivo*.

miR-24 affects the TGFβ pathway

Trb3-dependent regulation of Smurf1 not only stabilizes BMP-specific Smads but also TGFβ-specific Smads, Smad2 and Smad3 (Chan *et al*, 2007). Indeed we observed that PDGF stimulation decreases the level of Trb3 and Smad1 (Figure 2D, left panel), as well as Smad2 and Smad3, in PASMCs (Figure 2D, right panel). Thus, we speculated that miR-24 might negatively regulate the TGFβ-signalling pathway. Overexpression of miR-24 decreased total Smad2 and Smad3, as well as Trb3 protein level and abolished the TGFβ-mediated phosphorylation of Smad2 (Figure 9A), similar to the observation with the BMP-specific Smad (see Figure 6A). This result suggests that miR-24 is able to inhibit the TGFβ−Smad-signalling pathway. The mink lung epithelial cell line Mv1Lu was transfected with a luciferase-reporter construct (SBE-Luc), which contained four copies of the Smad DNA-binding element (SBE). Induction of the SBE-Luc reporter by TGFβ treatment was dramatically reduced by miR-24 mimic (Figure 9B), suggesting that miR-24 inhibits the TGFβ–Smad-signalling pathway. To examine whether miR-24-mediated inhibition of SBE-Luc reporter activity is due to downregulation of Trb3, Trb3 expression constructs with or without the 3′-UTR (see Figure 3C, top panel) were co-transfected with miR-24 mimic. A similar level of Trb3 mRNA was expressed from both constructs in Mv1Lu cells (Figure 9C, right panel). The inhibitory effect of miR-24 mimic was absent when Trb3 construct lacking the 3′-UTR was co-transfected, presumably because Trb3 mRNA expressed from this construct is resistant to miR-24 (Figure 9C, left panel, Trb3). In contrast, the Trb3 construct with the 3′-UTR was unable to rescue the inhibitory activity of the miR-24 mimic (Figure 9C, left panel, Trb3 + 3′-UTR), suggesting that inhibition of the TGFβ–Smad pathway by miR-24 requires targeting of Trb3 by miR-24. The TGFβ–Smad-signalling pathway induces the expression of contractile genes in vSMCs in a Smad-dependent manner (Lagna *et al*, 2007). We examined the effect of Trb3 downregulation

Figure 6 miR-24 inhibits BMP signalling in vSMCs through downregulation of Trb3 (**A**). PASMCs were transfected with 0.3 nM Control mimic or 0.3 nM miR-24 mimic. Twenty-four hours after transfection of mimic, cells were stimulated with 3 nM BMP4 for 2 h and subjected to immunoblot analysis using anti-Trb3, anti-Smad1, anti-phospho-Smad1/5 (Pi-Smad1/5), or anti-GAPDH antibody (loading control). The experiment was repeated twice and produced similar results. (**B**) PASMCs were transfected with 0.1 nM miR-24 mimic or control mimic, followed by stimulation with 3 nM BMP4 (+BMP4) for 6 h (Id3) or for 24 h (all other markers). qRT–PCR was then performed. Relative expression of SMA, Id3, and Trb3 normalized to GAPDH and miR-24 expression normalized to U6 snRNA are plotted (means ± s.e.m., $n=3$; $^*P<0.001$). (**C**) PASMCs were transfected with 0.3 nM miR-24 mimic or control mimic, followed by adenoviral transduction of the Trb3 expression construct (Trb3 (WT) or Trb3 (ΔK)), or adenoviral transduction of GFP expression construct as control. Twenty-four hours later stimulation with 3 nM BMP4 was performed for 6 h for Id3 or 24 h for SMA. qRT–PCR was then performed and relative expression of SMA, Id3, and Trb3 normalized to GAPDH and miR-24 expression normalized to U6 snRNA are plotted (means ± s.e.m., $n=3$; $^*P<0.001$). (**D**) PASMCs were transfected with 0.3 nM control mimic or miR-24 mimic (left panel) for 24 h, followed by stimulation with 3 nM BMP4 (+BMP4) for 4 h. qRT–PCR was then performed to determine relative expression of miR-21 normalized to U6 snRNA and Trb3 expression normalized to GAPDH (means ± s.e.m., $n=3$; $^*P<0.001$). (**E**) PASMCs were transfected with 50 nM si-Control or si-Trb3 (right panel) for 24 h, followed by stimulation with 3 nM BMP4 (+BMP4) for 4 h. qRT–PCR was then performed to determine relative expression of miR-21 normalized to U6 snRNA and Trb3 expression normalized to GAPDH (means ± s.e.m., $n=3$; $^*P<0.001$). (**F**) PASMCs were transfected with 3 nM control mimic (control) or miR-24 mimic (miR-24 mimic) for 24 h, placed in starvation media for 24 h, followed by stimulation with BMP4 (+BMP4) for 48 h. Cells were trypsinized and counted using a haemocytometer. The relative number of cells is plotted means ± s.e.m. ($n=3$); $^*P<0.001$ (compared with unstimulated). (**G**) PASMCs were transfected with 3 nM control mimic (control) or miR-24 mimic (miR-24 mimic) for 24 h, followed by stimulation with BMP4 (+BMP4) for 24 h or left unstimulated (none). PASMCs were then embedded to collagen gel lattices with continued stimulation. Twenty-four hours after the collagen lattices were dissociated from the dish, gel contraction was photographed by using a digital camera (left panel). The relative size of collagen gel was quantitated using ImageJ and is plotted (means ± s.e.m., $n=3$; $^*P<0.001$, compared with unstimulated condition (right panel)). (**H**) A clone of P19 cells, stably transfected with the BMP reporter construct BRE-Luc, was transfected with 3 nM control mimic, 0.3 nM or 3 nM miR-24 mimic, or 50 nM si-Trb3, followed by 24-h BMP4 treatment. Luciferase activity was then measured and fold induction of the activity after BMP4 treatment is plotted (means ± s.e.m., $n=3$; $^*P<0.001$, compared with control mimic). (**I**) C2C12 cells were transfected with 0.003 nM control mimic (control) or 0.003 nM miR-24 mimic (miR-24) for 24 h followed by stimulation with BMP4 (+BMP4) for 2 h, or left unstimulated (none). qRT–PCR was then performed. Relative expression of ALP, Id3, and Trb3 normalized to GAPDH and miR-24 expression normalized to U6 snRNA are plotted (means ± s.e.m., $n=3$; $^*P<0.001$).

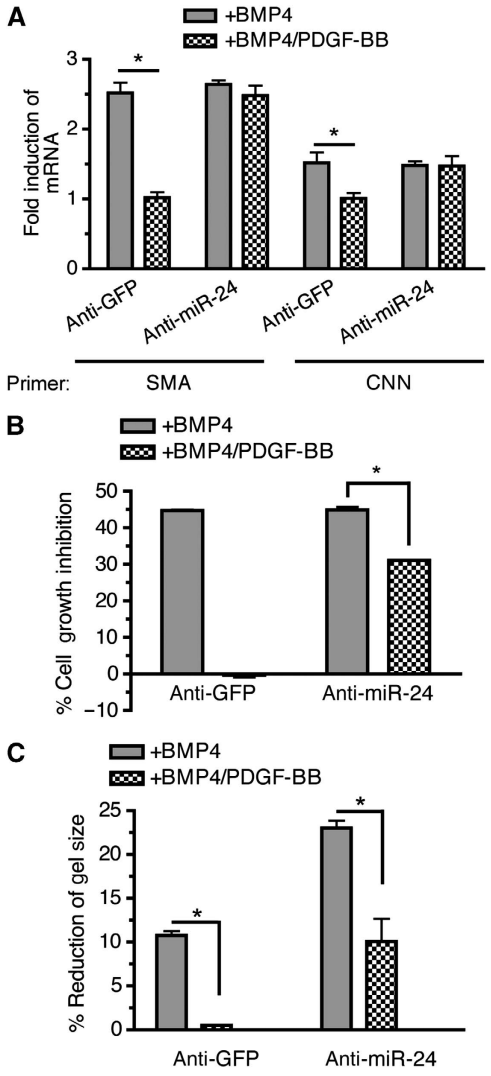

Figure 7 miR-24 expression is essential for PDGF-BB inhibition of the BMP-mediated contractile phenotype in PASMCs. PASMCs were transfected with 50 nM anti-GFP (control) or anti-miR-24 for 24 h prior to stimulation with 3 nM BMP4, 20 ng/ml PDGF-BB, or both, as indicated. (**A**) qRT–PCR anaylses of SMA and CNN were performed. The fold induction of SMA mRNA (compared with no stimulation) is plotted; error bars represent s.e.m. ($n=3$); $^*P<0.001$. (**B**) Cells were trypsinized and counted using a haemocytometer. The percentage of cell growth inhibition is plotted as means ± s.e.m. ($n=3$); $^*P<0.001$. (**C**) Cells were embedded in collagen gel lattices and treated with 3 nM BMP4 alone (+BMP4), or 3 nM BMP4 and 20 ng/ml PDGF-BB (+BMP4/PDGF-BB). Twenty-four hours after the collagen lattices were dissociated from the dish, percentage reduction of gel size as compared with the no stimulation condition was measured and is plotted (means ± s.e.m., $n=3$; $^*P<0.001$).

on contractile gene expression in vSMCs. Endogenous Trb3 was downregulated by siRNA (si-Trb3) in PASMCs and the levels of contractile markers (SMA, CNN, and SM22), as well as the well-characterized TGFβ–Smad-target gene, plasminogen activator inhibitor-1 (PAI-1), were examined after TGFβ treatment (Figure 9D). TGFβ treatment induced all three vSMC markers and PAI-1 expression (Figure 9D). However, in si-Trb3-transfected cells in which Trb3 level was reduced to ~30% of endogenous level, not only PAI-1 but also vSMC markers could not be augmented by TGFβ (Figure 9D). This result confirms that Trb3 is essential for induction of vSMC markers by TGFβ, presumably because Trb3 critically regulates the protein stability of TGFβ-specific Smads. Next the effect of miR-24 overexpression on TGFβ-mediated induction of vSMC genes and miR-21 was examined. The expression of exogenous miR-24 ~3-fold over the endogenous level (see Figure 9E, right panel, miR-24) reduced Trb3 mRNA to ~20% of the endogenous level (Figure 9E, left panel, Trb3). Similar to the result in Figure 9D using si-Trb3-transfected cells, both the basal and the TGFβ-induced level of contractile markers SMA and CNN were significantly reduced by elevation of miR-24 expression (Figure 9E, left panel). Induction of miR-21 upon TGFβ stimulation was also abolished in the presence of miR-24 mimic (Figure 9E, right panel, miR-21). These results suggest that miR-24 negatively regulates the TGFβ–Smad signal via silencing Trb3, followed by downregulation of Smad signal transducers. Finally, induction of vSMC-specific genes by TGFβ was inhibited by co-treatment with PDGF-BB (Figure 9F), as shown for the BMP4 pathway (Figure 7A). Trb3 mRNA was also decreased by TGFβ/PDGF-BB co-treatment. Inhibition of TGFβ-induced contractile genes, as well as Trb3, by PDGF-BB was blocked when miR-24 was inhibited by anti-miR-24 (Figure 9F), suggesting that PDGF-BB interferes with the pro-contractile TGFβ signal by modulating Trb3 and Smads level via induction of miR-24 (Figure 9F). Altogether, these results demonstrate that miR-24 plays a critical role in the regulation of the vSMC phenotype switch by antagonizing pro-contractile signals by members of the TGFβ superfamily of signalling pathways, as summarized in Figure 9G.

Discussion

In this study, we elucidated a novel mechanism by which PDGF-BB signal promotes the dedifferentiation of vSMCs. We demonstrated that PDGF-BB induces miR-24 and induces degradation of Trb3 mRNA, which in turn leads to downregulation of Smad signal transducers. The Smad proteins are essential mediators of the pro-contractile signal transmitted by BMP and TGFβ. miR-24 is clustered closely with miR-23 and miR-27 at two genomic loci known as the miR-24-1 gene cluster, an ~880-bp region encoding miR-23b, -27b, and -24-1, and the miR-24-2 gene cluster, a ~370-bp region encoding miR-23a, -27a, and -24-2. Our result indicates that all three miRNAs of the miR-24-2 cluster, but not the miR-24-1 cluster, are regulated to a similar extent by PDGF-BB at the level of primary transcripts, suggesting that the miR-24-2 gene cluster is transcribed into a single transcript, which will then be processed into three independent miRNAs. Differential expression and regulation of miR-24-1 and miR-24-2 have been observed previously. In mouse mesenchymal C3H10T1/2 cells, BMP2 induces miR-24-1 expression without affecting the expression of miR-24-2 (Sun *et al*, 2009). Interestingly, miR-24-1 but not miR-23b or miR-27b encoded in the same gene locus are regulated by BMP2, suggesting that three miRNAs in the miR-24-1 cluster might be differentially regulated during processing. In mouse myoblast C2C12 cells, TGFβ was shown to repress miR-24-2, as well as miR-23a and miR-27a (Sun *et al*, 2008). We did not observe significant changes in the expression of miR-24 upon TGFβ or BMP stimulation, suggesting that neither the miR-24-1 nor the miR-24-2 cluster is regulated by TGFβ or BMP at the level

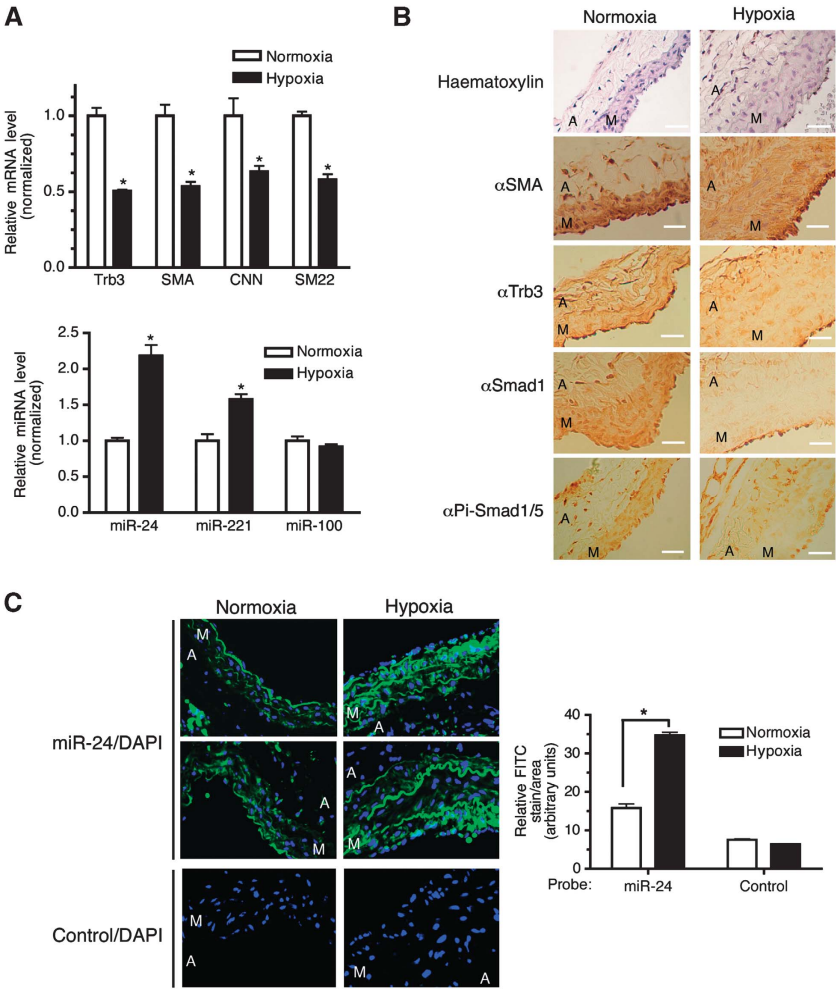

Figure 8 Modulation of Trb3 and miR-24 expression in a rat PAH model (**A**). qRT–PCR analysis of lung samples from rats after 17-day hypoxia or normoxia treatment. Relative expression of Trb3, SMA, CNN, and SM22 (top panel); or miR-24, miR-221, and miR-100 was plotted by normalizing the level of expression of normoxia samples as 1 (means ± s.e.m., $n=3$; $^*P<0.001$). (**B**) Histological examination of PAs from rats after 17-day hypoxia or normoxia treatment with anti-SMA, anti-Smad1, anti-phospho Smad1/5 (Pi-Smad1/5), or anti-Trb3 antibodies (brown, ×400) and by haematoxylin staining (blue, ×400). The media (M) and adventitia (A) of the PAs are indicated. (**C**) Sections of PAs were probed with either anti-miR-24 (top two panels) or control (bottom panel) conjugated to FITC (green). Cells were counterstained with DAPI (blue). The media (M) and adventitia (A) of the PAs are indicated. Relative expression of miR-24 was quantitated using the ImageJ software and imaged ($n=3$; $^*P<0.001$).

of transcription or processing in PASMCs. Thus, the mechanism of regulation of the miR-24 gene clusters by growth-factor-signalling pathways appears to be cell-type-specific. It will be interesting to investigate whether PDGF-BB-mediated transcriptional activation of the miR-24-2 cluster is limited to vSMCs.

Previously we showed that PDGF-BB signalling induces miR-221 in vSMCs and mediates downregulation of the c-Kit receptor and the cyclin-dependent kinase inhibitor p27Kip1 (Davis *et al*, 2009). Decreased expression of p27Kip1 promotes an increase in cell growth, while a decrease in c-Kit leads to inhibition of contractile gene markers by modulating the level of Myocd protein, a transcriptional activator critical for induction of contractile genes (Davis *et al*, 2009). We investigated a potential crosstalk between miR-221 and miR-24 activities by monitoring the effect of miR-221 overexpression on the level of Trb3 or miR-24, and found no evidence that miR-221 affects Trb3 or miR-24 expression (M Chun Chan and A Hata, unpublished observation). Conversely, overexpression of miR-24 did not affect the expression of miR-221 or the expression of its target genes (M Chun Chan and A Hata, unpublished observation). Furthermore, we observed that miR-24 does not play a role in regulating PDGF-BB-mediated migration (Supplementary Figure S4), an important characteristic of the synthetic phenotype. In comparison, we previously reported that the increase in miR-221 expression by PDGF-BB stimulation is required for vSMC migration (Davis *et al*, 2009). These observations suggest that miR-221 and miR-24 act independently to promote the synthetic phenotype in vSMCs despite their coordinated regulation by PDGF-BB.

We showed previously that BMP Smad-dependent signalling promotes nuclear translocation of MRTF-A and MRTF-B, members of the Myocd family with function similar to Myocd (Lagna *et al*, 2007). We speculate that nuclear accumulation of MRTF-A/B by BMP is inhibited by PDGF induction of miR-24 via Trb3-dependent downregulation of BMP–Smad signal transducers. Thus, it is intriguing to speculate that PDGF-BB might inhibit the expression of contractile markers by inhibiting the function of Myocd through induction of miR-221 and MRTF-A/B, through induction of miR-24.

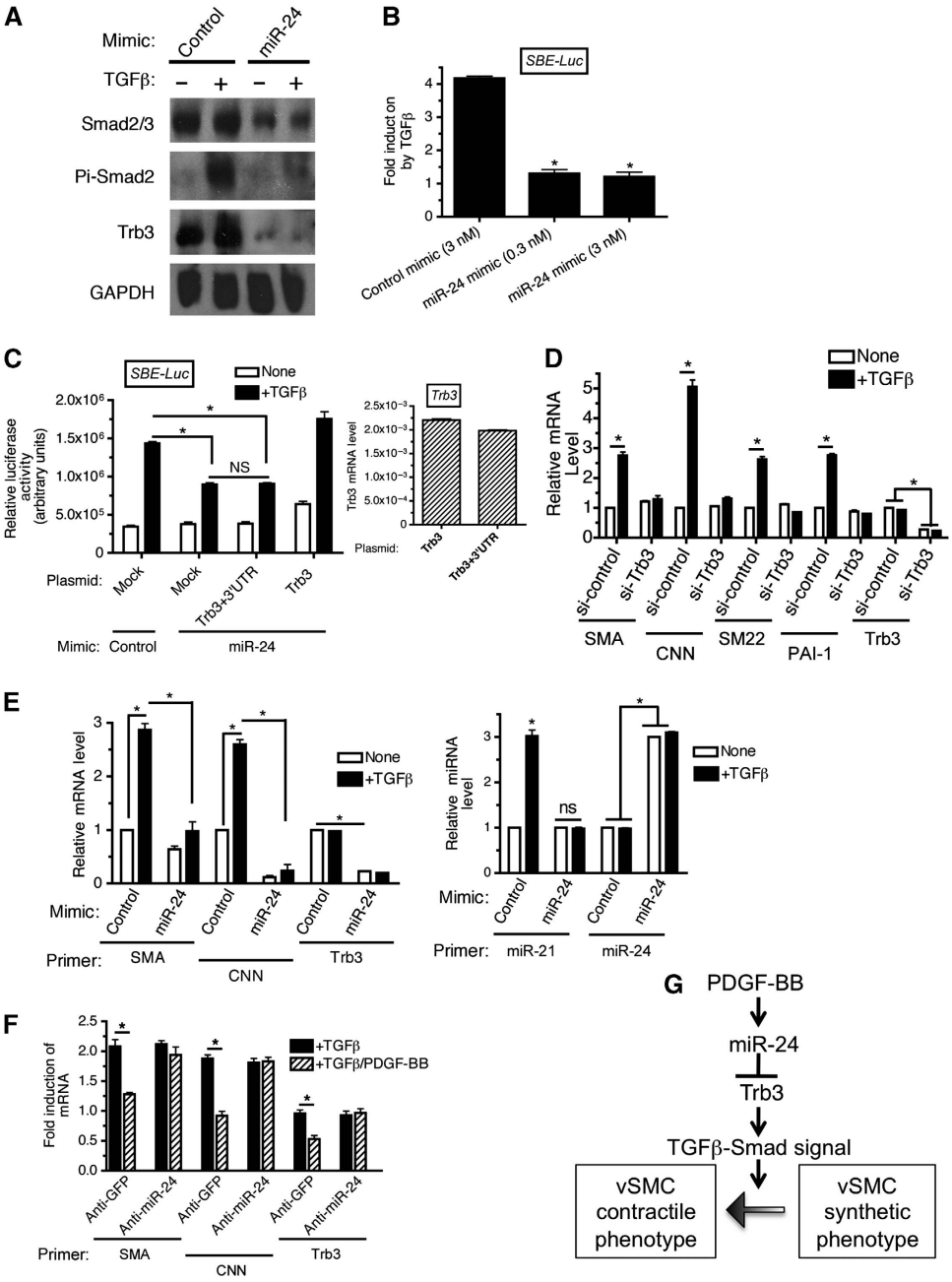

Figure 9 miR-24 antagonizes TGFβ signalling. (**A**) PASMCs were transfected with 0.3 nM Control mimic or 0.3 nM miR-24 mimic. Twenty-four hours after transfection of mimic, cells were stimulated with 100 pM TGFβ1 for 2 h and subjected to immunoblot analysis with anti-Trb3, anti-Smad2/3, anti-phospho-Smad2 (Pi-Smad2), or anti-GAPDH antibody (loading control). The experiment was repeated twice and produced similar results. (**B**) Mv1Lu cells were transfected with the TGFβ reporter construct SBE-Luc as well as with 3 nM control mimic, or 0.3 or 3 nM miR24 mimic. Cells were then stimulated with 100 pM TGFβ1 for 24 h and luciferase activities were measured. Results are plotted as fold induction upon TGFβ stimulation (means ± s.e.m., $n=3$; $^*P<0.001$), versus fold induction with control mimic). (**C**) Mv1Lu cells was transfected with SBE-Luc, 3 nM control mimic, or miR-24 mimic, as well as the Trb3 expression construct with the 3′-UTR containing the miR-24 seed sequence (Trb3 + 3′-UTR) or without the 3'UTR (Trb3). Cells were stimulated with 100 pM TGFβ1 for 24 h and luciferase activities were measured (means ± s.e.m., $n=3$). Relative exogenous Trb3 mRNA normalized to GAPDH in samples transfected with control mimic were monitored by qRT–PCR (right panel). (**D**) PASMCs were transfected with 50 nM si-Control or si-Trb3, followed by 100 pM TGFβ1 treatment for 24 h. qRT–PCR analysis of SMA, CNN, SM22, PAI-1, or Trb3 mRNA was performed. The relative mRNA levels normalized to GAPDH are plotted as means ± s.e.m. ($n=3$; $^*P<0.001$). (**E**) PASMCs were transfected with 3 nM control mimic (control), or miR-24 mimic, followed by 100 pM TGFβ1 treatment for 24 h. qRT–PCR analysis of SMA, CNN, or Trb3 mRNA, or miR-21 or miR-24 was performed. Relative mRNA levels normalized to GAPDH and miR-21 expression normalized to U6 snRNA were plotted as means ± s.e.m. ($n=3$; $^*P<0.001$). (**F**) PASMCs were transfected with 50 nM anti-GFP (control) or anti-miR-24 for 24 h. Cells were then treated with 100 pM TGFβ1 alone (+TGFβ) or both100 pM TGFβ1 and 20 ng/ml PDGF-BB (+TGFβ/PDGF-BB) for 24 h. qRT–PCR analysis for SMA, CNN, or Trb3 was performed and data of fold induction of mRNA as compared with unstimulated was plotted as means ± s.e.m. ($n=3$; $^*P<0.001$). (**G**) A schematic representation of the mechanism of antagonism between PDGF and the TGFβ-signalling pathway mediated by miR-24.

Our previous study demonstrates that miR-21 biosynthesis is facilitated by both the BMP- and TGFβ-signalling pathway (Davis *et al*, 2008). Upon translocation into the nucleus, Smads become part of a large Drosha microprocessor complex and facilitate cleavage and processing of Pri-miR-21 (Davis *et al*, 2008). Mature miR-21 downregulates PDCD4,

which in turn elevates contractile gene expression (Davis *et al*, 2008). In this study, we showed that modulation of miR-24 or Trb3 affects the induction of miR-21 by BMP4 (Figure 6D and E). Therefore, another mechanism by which miR-24 could mediate the inhibition of contractile genes is through increased levels of PDCD4 due to inhibition of miR-21 biogenesis.

We demonstrated antagonism between miR-24 and the TGFβ superfamily of signalling pathways in both vSMCs and non-vSMCs. In human hepatocellular carcinoma cells, consistent with our observation, increased expression of miR-24-2, miR-23a, and miR-27a has been suggested to change the TGFβ signal from being growth-inhibitory, proapoptotic to growth-stimulatory, antiapoptotic (Huang *et al*, 2008). Similarly, increased expression of miR-24 has been observed in various tumours, such as pancreatic adenocarcinomas, uterine leiomyomas, chromic lymphotic leukaemias, breast carcinomas, and cholangiocarcinomas (Mattie *et al*, 2006; Meng *et al*, 2006; Fulci *et al*, 2007; Lee *et al*, 2007; Wang *et al*, 2007). These results suggest that inhibition of TGFβ signalling by miR-24 might be a relatively common mechanism during tumorigenesis. Another example of the antagonistic activity of miR-24 on TGFβ-superfamily signalling is during erythropoiesis. miR-24 inhibits activin-dependent erythropoiesis by targeting the activin type-I receptor (also known as ALK4) gene (Wang *et al*, 2008). Furthermore, the antimyogenic activity of TGFβ is inhibited by elevated expression of miR-24 during skeletal muscle differentiation in myoblast C2C12 cells (Sun *et al*, 2008). In vSMCs, mRNA or protein levels of BMP or TGFβ receptors are not affected by miR-24 (data not shown). We identified Trb3 as a novel target of miR-24. We have shown previously that Trb3 mediates degradation of Smurf1 (Chan *et al*, 2007). Besides a role in degradation of Smads, Smurf1 is known to facilitate the antagonistic action of Smad7 by targeting Smad7 at the plasma membrane (Suzuki *et al*, 2002). Furthermore, Smurf1 promotes degradation of RhoA (Wang *et al*, 2006), which is a downstream signal transducer critical for mediating the pro-contractile signal from the BMP pathway in vSMCs (Chan *et al*, 2007; Lagna *et al*, 2007). Thus, we speculate that induction of miR-24 by PDGF-BB leads to inhibition of pro-contractile signals via multiple mechanisms through degradation of different effectors critical for the TGFβ- or BMP-signalling pathways.

Trb3 is known to interact and negatively regulate the transcription factor peroxisome proliferation-activated receptor-γ (PPARγ), a master regulator of adipogenesis (Takahashi *et al*, 2008). Concurrently, it has been shown that expression of Trb3, both at the mRNA and the protein level, is silenced during early adipogenesis (Bezy *et al*, 2007). Constitutive expression of Trb3 in preadipocytes blocks adipocyte differentiation, suggesting that downregulation of Trb3 is essential for adipogenesis (Bezy *et al*, 2007). Recently, it was reported that BMP2-mediated adipocyte differentiation in 10T1/2 cells is enhanced by overexpression of miR-24 (Sun *et al*, 2009). This observation is contradictory to our study as miR-24 inhibits BMP signalling in vSMCs. We do not know whether miR-24 causes downregulation of Smads in preadipocytes similar to vSMCs. However, we speculate that overexpression of miR-24 in 10T1/2 cells causes downregulation of Trb3, which in turn leads to activation of PPARγ and adipocyte differentiation.

Aberrant regulation of the vSMC phenotype, in particular the switch from a highly contractile to a less contractile, synthetic phenotype, is a critical phenomenon underlying the pathogenesis of a variety of vascular proliferative diseases, including PAH. In this study we confirm that PDGF signalling is a potent inducer of the synthetic phenotype and is able to oppose the contractile action of the BMP or TGFβ pathways, and propose that it acts via induction of miR-24. Increased expression of both PDGF ligands and receptors has been reported using PAH animal models, as well as for human patients (Andrae *et al*, 2008). The tyrosine-kinase inhibitor imatinib mesylate, which strongly antagonizes the PDGF-signalling pathway, is able to reverse the phenotype of experimental PAH in animal models and improve symptoms in human IPAH patients (Andrae *et al*, 2008), suggesting that increased PDGF signalling in vSMCs contributes to development of IPAH. Our result indicates that hypoxia induces miR-24 expression and downregulation of Trb3, suggesting that elevation of miR-24 might cause thickening of the medial layer as a result of inhibition of BMP signalling, similar to that in IPAH patients with BMPRII mutations. It is intriguing to speculate that the level of expression of miR-24 might be upregulated in the pulmonary vasculature of IPAH patients, in comparison with normal vasculature, with concurrent decrease in Trb3 expression. If aberrant expression of miR-24 in the vasculature of PAH or other cardiovascular diseases is confirmed, modulation of the miR-24 level *in vivo* by delivery of anti-miR-24 oligonucleotides could be considered a novel therapy.

Materials and methods

Cell culture

Human primary PASMCs were purchased from Lonza (#CC-2581) and were maintained in Sm-GM2 media (Lonza) containing 5% FBS. Early-passage (passage 4–7) PASMCs were used for this study. PAC1, C3H10T1/2, P19, mink lung epithelial (MV1Lu), and C2C12 cell lines were purchased from ATCC and maintained in Dulbecco's modified Eagle's medium supplemented with 10% fetal calf serum (FCS; Sigma). Recombinant human BMP4, PDGF-BB, and TGFβ1 were purchased from R&D Systems. Cells were treated with 3 nM BMP4, 20 ng/ml PDGF-BB, or 100 pM TGFβ1 alone or a combination of these factors under starvation conditions (0.2% FBS) as described (Lagna *et al*, 2007).

RNA preparation and real-time RT–PCR

Total RNA was extracted by TRIzol (Invitrogen). For detection of mRNAs, 1 μg of RNA was subjected to RT reaction using the first-strand cDNA synthesis kit (Invitrogen) according to the manufacturer's instructions. Quantitative analysis of the change in expression levels was performed using a real-time PCR machine (iQ5; Bio-Rad) PCR cycling conditions were 94°C for 3 min and 40 cycles of (94°C for 15 s, 60°C for 20 s, and 72°C for 40 s). For detection of mature miRNAs, the TaqMan MicroRNA assay kit (Applied Biosystems) was used according to the manufacturer's instructions. Data analysis was performed by comparative C_t method using the Bio-Rad software. The average of three experiments each performed in triplicate along with their standard errors are presented. The sequences of RT–PCR primers can be found in the Supplementary data.

miRNA mimic

Chemically modified double-stranded RNAs designed to mimic endogenous mature miR-24, miR-221, and negative-control miRNA were purchased from Ambion. miRNA mimics were transfected using RNAi Max (Invitrogen) according to the manufacturer's directions at 0.3 or 3 nM as indicated.

Anti-miRNA oligonucleotides
2′-*O*-methyl-modified RNA oligonucleotides complementary to the miRNA or GFP (control) sequence were purchased from IDT and transfected as previously reported (Davis *et al*, 2008, 2009).

RNA interference
Synthetic siRNAs targeting human Trb3 or mouse Trb3 were purchased from Dharmacon as described previously (Chan *et al*, 2007). An siRNA with a non-targeting sequence (scramble siRNA; Dharmacon) was used as negative control. The siRNAs were transfected at 50 nM using RNAi Max (Invitrogen) according to the manufacturer's directions. FITC-conjugated fluorescence oligonucleotides (Block-it; Invitrogen) were used to evaluate transfection efficiency.

Plasmid DNA transfection and cDNA expression constructs
Cells were transfected using Fugene6 (Roche) according to the manufacturer's protocol. Human Trb3 expression plasmid with the 3′-UTR was purchased from Origene (cat. no. SC112991). Full-length human Trb3 including the 2-kb 3′-UTR, which contains the miR-221-target sequence, was cloned into a pCMV6-XL4 vector. Human Trb3 expression plasmid without the 3′-UTR, SBE-Luc, BRE-Luc, Trb3-luc, and adenoviral Trb3 construct (Ad_Trb3), were previously described (Chan *et al*, 2007).

Immunoblot assay
Cells were lysed in TNE buffer and total cell lysates were separated by SDS–PAGE, transferred to PVDF membranes (Millipore), immunoblotted with antibodies, and visualized using an enhanced chemiluminescence detection system (Amersham Biosciences). Protein bands were quantitated by densitometry using the gel analysis software ImageJ (rsbweb.nih.gov/ij/). Antibodies used for immunoblotting were anti-GAPDH antibody (2E3-2E10; Abnova), anti phospho Smad1/5/8 (clone 47-258; Calbiochem), anti-Smad1 (Zymed), anti-Smad2/3 (#610843; BD Biosciences), anti-phospho-Smad2 (a kind gift from Dr ten Dijke), and anti-SMA (clone 1A4; Sigma). Anti-human and mouse Trb3 antibodies were previously described (Chan *et al*, 2007).

Immunofluorescence staining
PASMCs or PAC1 cells were fixed and permeabilized in a 50% acetone–50% methanol solution and stained using anti-SMA antibody (clone 1A4; Sigma) conjugated with FITC, anti-hTrb3 conjugated with Cy3, and 4′-6-diamidino-2-phenylindole (DAPI; Invitrogen).

Luciferase assay
The luciferase-reporter construct was transfected together with β-galactosidase (β-gal) plasmid as an internal transfection control. Luciferase assays were performed as described (Lagna *et al*, 2007).

Collagen matrix contraction assay
Collagen matrix contraction assay was performed as described in the Supplementary data (Neuman *et al*, 2009).

Animal study and immunohistochemistry
All experiments were performed in accordance with the guidelines and regulations of the Institutional Animal Care and Use Committee at Tufts Medical Center. Adult male Sprague–Dawley rats were randomized to 17 days of normoxia or hypobaric hypoxia as described previously (Preston *et al*, 2006). At the end of the exposure period, rats were killed and PAs were processed for paraffin embedding. Paraffin-embedded tissue sections (5-μm) were immunostained as described in the Supplementary data.

In situ hybridization of miRNA
Rat PA sections were hybridized with a miRCURY LNA detection probe for miR-24 (cat. no. 18121-01; Exiqon) or with a control scrambled control probe (cat. no. 99004-01; Exiqon), followed by treatment with anti-DIG-HRP antibody (antibody 6212; Abcam) and signal amplification by Tyramide Technology from Molecular Probes (Invitrogen).

Statistical analysis
The results presented are the average of at least three experiments each performed in triplicate along with the standard errors. Statistical analyses were performed by analysis of variance, followed by Tukey's multiple comparison test or Student's *t*-test as appropriate, using Prism 4 (GraphPad Software Inc.). *P*-values less than 0.05 were considered significant and are indicated by asterisks.

Supplementary data
Supplementary data are available at *The EMBO Journal* Online (http://www.embojournal.org).

Acknowledgements
We thank Dr P ten Dijke for antibodies and R Warburton and F Celestin for technical assistance. We also thank the members of the Hata and Lagna laboratory for critical discussion. This work was supported by grants from the National Institutes of Health (HD042149 and HL082854) to AH and (HL086572) to GL. M-CC is a recipient of a postdoctoral fellowship from the American Heart Association.

Conflict of interest
The authors declare that they have no conflict of interest.

References
Andrae J, Gallini R, Betsholtz C (2008) Role of platelet-derived growth factors in physiology and medicine. *Genes Dev* **22:** 1276–1312

Bezy O, Vernochet C, Gesta S, Farmer SR, Kahn CR (2007) TRB3 blocks adipocyte differentiation through the inhibition of C/EBPbeta transcriptional activity. *Mol Cell Biol* **27:** 6818–6831

Bowers AJ, Scully S, Boylan JF (2003) SKIP3, a novel *Drosophila* tribbles ortholog, is overexpressed in human tumors and is regulated by hypoxia. *Oncogene* **22:** 2823–2835

Chan MC, Nguyen PH, Davis BN, Ohoka N, Hayashi H, Du K, Lagna G, Hata A (2007) A novel regulatory mechanism of the bone morphogenetic protein (BMP) signaling pathway involving the carboxyl-terminal tail domain of BMP type II receptor. *Mol Cell Biol* **27:** 5776–5789

Davidson AJ, Zon LI (2000) Turning mesoderm into blood: the formation of hematopoietic stem cells during embryogenesis. *Curr Top Dev Biol* **50:** 45–60

Davis BN, Hilyard AC, Lagna G, Hata A (2008) SMAD proteins control DROSHA-mediated microRNA maturation. *Nature* **454:** 56–61

Davis BN, Hilyard AC, Nguyen PH, Lagna G, Hata A (2009) Induction of microRNA-221 by platelet-derived growth factor signaling is critical for modulation of vascular smooth muscle phenotype. *J Biol Chem* **284:** 3728–3738

Fulci V, Chiaretti S, Goldoni M, Azzalin G, Carucci N, Tavolaro S, Castellano L, Magrelli A, Citarella F, Messina M, Maggio R, Peragine N, Santangelo S, Mauro FR, Landgraf P, Tuschl T, Weir DB, Chien M, Russo JJ, Ju J *et al* (2007) Quantitative technologies establish a novel microRNA profile of chronic lymphocytic leukemia. *Blood* **109:** 4944–4951

Guo J, Sartor M, Karyala S, Medvedovic M, Kann S, Puga A, Ryan P, Tomlinson CR (2004) Expression of genes in the TGF-beta signaling pathway is significantly deregulated in smooth muscle cells from aorta of aryl hydrocarbon receptor knockout mice. *Toxicol Appl Pharmacol* **194:** 79–89

Huang S, He X, Ding J, Liang L, Zhao Y, Zhang Z, Yao X, Pan Z, Zhang P, Li J, Wan D, Gu J (2008) Upregulation of miR-23a ~27a ~24 decreases transforming growth factor-beta-induced tumor-suppressive activities in human hepatocellular carcinoma cells. *Int J Cancer* **123:** 972–978

Ku M, Howard S, Ni W, Lagna G, Hata A (2005) OAZ regulates BMP signaling through SMAD6 activation. *J Biol Chem* **281:** 5277–5287

Kuwahara K, Teg Pipes GC, McAnally J, Richardson JA, Hill JA, Bassel-Duby R, Olson EN (2007) Modulation of adverse cardiac remodeling by STARS, a mediator of MEF2 signaling and SRF activity. *J Clin Invest* **117:** 1324–1334

Lagna G, Ku MM, Nguyen PH, Neuman NA, Davis BN, Hata A (2007) Control of phenotypic plasticity of smooth muscle cells by BMP signaling through the myocardin-related transcription factors. *J Biol Chem* **282:** 37244–37255

Lee EJ, Gusev Y, Jiang J, Nuovo GJ, Lerner MR, Frankel WL, Morgan DL, Postier RG, Brackett DJ, Schmittgen TD (2007) Expression profiling identifies microRNA signature in pancreatic cancer. *Int J Cancer* **120:** 1046–1054

Li S, Chang S, Qi X, Richardson JA, Olson EN (2006) Requirement of a myocardin-related transcription factor for development of mammary myoepithelial cells. *Mol Cell Biol* **26:** 5797–5808

Mattie MD, Benz CC, Bowers J, Sensinger K, Wong L, Scott GK, Fedele V, Ginzinger D, Getts R, Haqq C (2006) Optimized high-throughput microRNA expression profiling provides novel biomarker assessment of clinical prostate and breast cancer biopsies. *Mol Cancer* **5:** 24

McNamara CA, Sarembock IJ, Bachhuber BG, Stouffer GA, Ragosta M, Barry W, Gimple LW, Powers ER, Owens GK (1996) Thrombin and vascular smooth muscle cell proliferation: implications for atherosclerosis and restenosis. *Semin Thromb Hemost* **22:** 139–144

Medjkane S, Perez-Sanchez C, Gaggioli C, Sahai E, Treisman R (2009) Myocardin-related transcription factors and SRF are required for cytoskeletal dynamics and experimental metastasis. *Nat Cell Biol* **11:** 257–268

Meng F, Henson R, Lang M, Wehbe H, Maheshwari S, Mendell JT, Jiang J, Schmittgen TD, Patel T (2006) Involvement of human micro-RNA in growth and response to chemotherapy in human cholangiocarcinoma cell lines. *Gastroenterology* **130:** 2113–2129

Misiakos EP, Kouraklis G, Agapitos E, Perrea D, Karatzas G, Boudoulas H, Karayannakos PE (2001) Expression of PDGF-A, TGFb and VCAM-1 during the developmental stages of experimental atherosclerosis. *Eur Surg Res* **33:** 264–269

Monzen K, Nagai R, Komuro I (2002) A role for bone morphogenetic protein signaling in cardiomyocyte differentiation. *Trends Cardiovasc Med* **12:** 263–269

Moser M, Patterson C (2005) Bone morphogenetic proteins and vascular differentiation: BMPing up vasculogenesis. *Thromb Haemost* **94:** 713–718

Neuman NA, Ma S, Schnitzler GR, Zhu Y, Lagna G, Hata A (2009) The four-and-a-half LIM domain protein 2 regulates vascular smooth muscle phenotype and vascular tone. *J Biol Chem* **284:** 13202–13212

Ohoka N, Yoshii S, Hattori T, Onozaki K, Hayashi H (2005) TRB3, a novel ER stress-inducible gene, is induced via ATF4–CHOP pathway and is involved in cell death. *EMBO J* **24:** 1243–1255

Owens G (1995) Regulation of differentiation of vascular smooth muscle cells. *Physiol Rev* **75:** 487–517

Owens GK, Kumar MS, Wamhoff BR (2004) Molecular regulation of vascular smooth muscle cell differentiation in development and disease. *Physiol Rev* **84:** 767–801

Preston IR, Hill NS, Warburton RR, Fanburg BL (2006) Role of 12-lipoxygenase in hypoxia-induced rat pulmonary artery smooth muscle cell proliferation. *Am J Physiol Lung Cell Mol Physiol* **290:** L367–L374

Qi L, Heredia JE, Altarejos JY, Screaton R, Goebel N, Niessen S, Macleod IX, Liew CW, Kulkarni RN, Bain J, Newgard C, Nelson M, Evans RM, Yates J, Montminy M (2006) TRB3 links the E3 ubiquitin ligase COP1 to lipid metabolism. *Science* **312:** 1763–1766

Schneider MD, Gaussin V, Lyons KM (2003) Tempting fate: BMP signals for cardiac morphogenesis. *Cytokine Growth Factor Rev* **14:** 1–4

Smith P, Heath D, Yacoub M, Madden B, Caslin A, Gosney J (1990) The ultrastructure of plexogenic pulmonary arteriopathy. *J Pathol* **160:** 111–121

Sun F, Wang J, Pan Q, Yu Y, Zhang Y, Wan Y, Li X, Hong A (2009) Characterization of function and regulation of miR-24-1 and miR-31. *Biochem Biophys Res Commun* **380:** 660–665

Sun Q, Zhang Y, Yang G, Chen X, Cao G, Wang J, Sun Y, Zhang P, Fan M, Shao N, Yang X (2008) Transforming growth factor-beta-regulated miR-24 promotes skeletal muscle differentiation. *Nucleic Acids Res* **36:** 2690–2699

Suzuki C, Murakami G, Fukuchi M, Shimanuki T, Shikauchi Y, Imamura T, Miyazono K (2002) Smurf1 regulates the inhibitory activity of Smad7 by targeting Smad7 to the plasma membrane. *J Biol Chem* **277:** 39919–39925

Takahashi Y, Ohoka N, Hayashi H, Sato R (2008) TRB3 suppresses adipocyte differentiation by negatively regulating PPARgamma transcriptional activity. *J Lipid Res* **49:** 880–892

ten Dijke P, Arthur HM (2007) Extracellular control of TGFb signalling in vascular development and disease. *Nature Rev Mol Cell Biol* **8:** 857–868

Wang HR, Ogunjimi AA, Zhang Y, Ozdamar B, Bose R, Wrana JL (2006) Degradation of RhoA by Smurf1 ubiquitin ligase. *Methods Enzymol* **406:** 437–447

Wang Q, Huang Z, Xue H, Jin C, Ju XL, Han JD, Chen YG (2008) MicroRNA miR-24 inhibits erythropoiesis by targeting activin type I receptor ALK4. *Blood* **111:** 588–595

Wang T, Zhang X, Obijuru L, Laser J, Aris V, Lee P, Mittal K, Soteropoulos P, Wei JJ (2007) A micro-RNA signature associated with race, tumor size, and target gene activity in human uterine leiomyomas. *Genes Chromosomes Cancer* **46:** 336–347

Yang X, Long L, Southwood M, Rudarakanchana N, Upton PD, Jeffery TK, Atkinson C, Chen H, Trembath RC, Morrell NW (2005) Dysfunctional Smad signaling contributes to abnormal smooth muscle cell proliferation in familial pulmonary arterial hypertension. *Circ Res* **96:** 1053–1063

Yi ES, Kim H, Ahn H, Strother J, Morris T, Masliah E, Hansen LA, Park K, Friedman PJ (2000) Distribution of obstructive intimal lesions and their cellular phenotypes in chronic pulmonary hypertension. A morphometric and immunohistochemical study. *Am J Respir Crit Care Med* **162** (4 Part 1)**:** 1577–1586

Yoshida T, Gan Q, Shang Y, Owens GK (2007) Platelet-derived growth factor-BB represses smooth muscle cell marker genes via changes in binding of MKL factors and histone deacetylases to their promoters. *Am J Physiol Cell Physiol* **292:** C886–C895